



**HAL**  
open science

## Effect of DNA repair inhibitor AsiDNA on the incidence of telomere fusion in crisis

Chloé Subecz, Jian-Sheng Sun, Lauréline Roger

### ► To cite this version:

Chloé Subecz, Jian-Sheng Sun, Lauréline Roger. Effect of DNA repair inhibitor AsiDNA on the incidence of telomere fusion in crisis. *Human Molecular Genetics*, 2021, 30 (3-4), pp.172-181. 10.1093/hmg/ddab008 . mnhn-03879689

**HAL Id: mnhn-03879689**

**<https://mnhn.hal.science/mnhn-03879689>**

Submitted on 6 Dec 2022

**HAL** is a multi-disciplinary open access archive for the deposit and dissemination of scientific research documents, whether they are published or not. The documents may come from teaching and research institutions in France or abroad, or from public or private research centers.

L'archive ouverte pluridisciplinaire **HAL**, est destinée au dépôt et à la diffusion de documents scientifiques de niveau recherche, publiés ou non, émanant des établissements d'enseignement et de recherche français ou étrangers, des laboratoires publics ou privés.



Distributed under a Creative Commons Attribution 4.0 International License

GENERAL ARTICLE

# Effect of DNA repair inhibitor AsiDNA on the incidence of telomere fusion in crisis

Chloé Subecz, Jian-Sheng Sun and Lauréline Roger\*

Structure and Instability of Genomes laboratory, “Muséum National d’Histoire Naturelle” (MNHN), Inserm U1154, CNRS UMR 7196, Paris, France

\*To whom correspondence should be addressed at: Muséum National d’Histoire Naturelle, Structure et Instabilité des Génomes, CNRS UMR 7196/INSERM U1154, 43 rue Cuvier - Case postale 26, 75231 Paris Cedex 05, France. Tel: +33(0)140793684; Fax: +33(0)140793705; Email: lroger@mnhn.fr

## Abstract

Telomere fusions lead to a state of genomic instability, and are thought to drive clonal evolution and tumorigenesis. Telomere fusions occur via both Classical and Alternative Non-Homologous End Joining repair pathways. AsiDNA is a DNA repair inhibitor that acts by mimicking a DNA double strand break (DSB) and hijacking the recruitment of proteins involved in various DNA repair pathways. In this study, we investigated whether the inhibition of DSB-repair pathways by AsiDNA could prevent telomere fusions during crisis. The present study showed that AsiDNA decreased the frequency of telomere fusions without affecting the rate of telomere erosion. Further, it indicated that AsiDNA does not impact the choice of the repair pathway used for the fusion of short dysfunctional telomeres. AsiDNA is thought to prevent short telomeres from fusing by inhibiting DNA repair. An alternative, non-mutually exclusive possibility is that cells harbouring fusions preferentially die in the presence of AsiDNA, thus resulting in a reduction in fusion frequency. This important work could open the way for investigating the use of AsiDNA in the treatment of tumours that have short dysfunctional telomeres and/or are experiencing genomic instability.

## Introduction

Telomeres are nucleoprotein structures that cap and protect the natural ends of linear chromosomes (1,2). One of their main functions is to prevent chromosome extremities from being recognized as DNA double strand breaks (DSB) by the DNA repair machinery (3). In human somatic cells, telomerase, the enzyme that regulates telomere length, is not expressed and telomeres shorten at each cell division because of the incomplete replication of linear chromosomes. Telomere erosion ultimately leads to a partial loss of telomere function and triggers a p53/Rb-dependent stable cell cycle arrest, called senescence (3). In the absence of fully functional DNA damage check-points, telomeres keep shortening, with ongoing cell divisions, up to a length at which they become dysfunctional and can fuse with other telomeres or non-telomeric loci (4–6). Telomere fusions lead to the formation of dicentric chromosomes and anaphase bridges

that initiate cycles of breakage-fusions-bridge resulting in a state of genomic instability, known as telomere crisis (7). Telomere crisis is characterized by slower cell growth and massive cell death, thus creating a selective pressure for the clonal outgrowth of rare cells that manage to maintain their telomere length, either by reactivation of telomerase expression or by activation of an alternative pathway (8).

Telomere crisis is thought to drive genomic instability and contribute to tumorigenesis. Indeed, in mouse models, telomere dysfunction is associated with the development of carcinomas containing chromosomal rearrangements similar to those observed in cells in crisis (9). Moreover, studies of telomere dynamics in solid and blood cancers in humans also suggest a role of telomere dysfunction in the initiation of tumorigenesis (10–12) and short telomere length is a poor prognostic factor in several cancers (13–17).

Received: September 21, 2020. Revised: December 12, 2020. Accepted: December 31, 2020

© The Author(s) 2021. Published by Oxford University Press.

This is an Open Access article distributed under the terms of the Creative Commons Attribution Non-Commercial License (<http://creativecommons.org/licenses/by-nc/4.0/>), which permits non-commercial re-use, distribution, and reproduction in any medium, provided the original work is properly cited. For commercial re-use, please contact [journals.permissions@oup.com](mailto:journals.permissions@oup.com)

Thus, inhibiting the repair of short dysfunctional telomeres in order to prevent telomere fusions and reduce genomic instability could be an interesting therapeutic avenue to limit cancer progression.

Both Classical (C-NHEJ) and Alternative (A-NHEJ) Non-Homologous End Joining repair pathways are involved in fusions between short dysfunctional telomeres (8). In C-NHEJ DNA blunt-ends are ligated. Core components of C-NHEJ include: the Ku complex that binds to DNA ends and initiates the repair process, DNA-dependant kinase catalytic subunit (DNA-PKcs), which is recruited by Ku to form the DNA-PK complex, and Ligase 4 which is responsible for the end ligation step (18). A-NHEJ uses >1 nt microhomologies flanking the DSB to align DNA ends before joining and is associated with large deletions and in some cases insertions at the repair junction. A-NHEJ core components include: Poly-ADP-Ribose-Polymerase 1 (PARP1), which binds DNA ends, Polymerase  $\theta$ , and Ligase 3, or to a lesser extent Ligase 1, for the end ligation (18).

AsiDNA is an oligonucleotide-based inhibitor that targets several DSB repair pathways including C-NHEJ and homologous recombination (HR) (19,20). AsiDNA is formed by two complementary 32-nucleotide strands connected by a linker and a cholesterol group at the 5'-end to allow direct cell delivery (21). AsiDNA mimics a DSB and hyper-activates PARP and DNA-PK thus preventing the targeted recruitment of repair proteins at the real damage site (19,20). The persistence of unrepaired DNA breaks leads to cell death. *In vitro*, AsiDNA is toxic to several cancer cell lines but not to normal cells (22). *In vivo*, in xenograft mouse models, AsiDNA has been shown to reduce tumour growth and increase survival (23) as well as to sensitize tumours to chemotherapy and radiotherapy (24). AsiDNA also exhibited promising results in phase 1 clinical trial in combination with radiotherapy to treat patients with skin metastasis from melanomas (25).

In this study, we investigated whether the inhibition of DSB-repair pathways by AsiDNA could prevent telomere fusions during crisis, thus limiting clonal selection and the emergence of cancer cells with a rearranged genome.

## Results

### Impact of AsiDNA on a telomere-driven crisis

In order to study the impact of AsiDNA on telomere fusions during crisis, we used a previously described model of colorectal cancer cell line expressing a dominant negative telomerase construct (HCT116-DNhTERT) (8). Due to telomerase inhibition, telomere shortening takes place at each cell division, and when telomeres become dysfunctional HCT116-DNhTERT cells enter in a crisis-like state characterized by telomere fusions, slower cell growth and increased cell death (8). This telomere crisis-like state is followed by telomerase reactivation, telomere lengthening, and the abrogation of telomere fusions (8).

As AsiDNA is toxic to cancer cells, we treated two independent clones of HCT116-DNhTERT with a sublethal concentration of AsiDNA at each passage (every 3–4 days) during the entire course of the experiment (Fig. 1A). We followed untreated cells as controls. As previously described (8), both untreated clones showed progressive telomere erosion as exemplified by Single Telomere Length Analysis (STELA) on 17p and XpYp chromosomes (Fig. 1B and Supplementary Material, Fig. S1) and entered crisis after approximately 15–19 PDs and 31–36 PDs respectively (Fig. 1A and B and Supplementary material, Fig. S1). At this point, telomere length stabilized despite cell divisions. Telomere crisis

was characterized by slow cell growth, a change in morphology, short telomeres, and increased telomere fusions (Fig. 1A–D and Supplementary Material, Fig. S1). Fusion events were very rarely observed out of crisis. After 25 and 27 days in crisis respectively some cells from both clones escaped crisis and kept growing until the experiment was ended (Fig. 1A).

AsiDNA hyper-activates DNA PK, which in turn phosphorylates the histone variant H2AX at serine 139. Typically, cells treated with AsiDNA are characterized by a pan-nuclear phosphorylation of H2AX. First, we confirmed the efficacy of AsiDNA by comparing H2AX phosphorylation in treated and untreated HCT116-DNhTERT cells by immunofluorescence. Treated cells harboured a pan-nuclear  $\gamma$ -H2AX (H2AX phosphorylated form) staining at all the day points analysed (i.e. before crisis, during crisis, and after crisis) (Fig. 2A and B and Supplementary Material, Fig. S2). In crisis, unprotected chromosome ends are recognized as DSBs leading to the activation of the DNA damage response and H2AX phosphorylation (26). In the treated cells in crisis, few  $\gamma$ -H2AX foci remained in addition to the pan-nuclear phosphorylation (Fig. 2A).

In both clones tested, the toxicity of AsiDNA in treated cells was evidenced by a decrease in population doublings compared with untreated controls (Fig. 1A). However treated cells behaved similarly to untreated cells, as they entered crisis after the same number of days in culture (around days 11–15 for clone 4 and 25–29 for clone 8, Fig. 1A) and managed to escape crisis. Noteworthy, in clone 8, the treated cells that escaped crisis seemed more sensitive to AsiDNA as they appeared to grow more slowly than the treated cells prior to crisis (growth rate of 0.60 PDs/days versus 0.93 PDs/days) (Fig. 1A).

### AsiDNA decreases the frequency of telomere fusions without affecting the rate of telomere erosion

We next examined whether AsiDNA has an impact on telomere erosion in HCT116-DNhTERT cells. In order to do so, we compared telomere length distributions in treated and untreated cells at several time points using STELA at 17p and XpYp telomeres in both clones (Fig. 3A, B and Supplementary material, Fig. S3). Telomeres shortened from an average length of 1.9 kb and 2.7 kb for clone 4 and 8 respectively at 17p telomere (1.1 kb and 2.9 kb at XpYp) to ~1.4–1.3 kb and 1.7–1.65 kb (0.6–0.5 kb and 1–0.9 kb at XpYp) at the beginning of crisis where telomere length stabilized. For both the clones, 17p and XpYp telomeres reached a lower limit of ~400–300 bp at the beginning of crisis, as previously described (8). At every time point examined in both clones, there was no statistical difference in the mean telomere length at 17p and XpYp between treated and untreated cells (Fig. 3B and Supplementary material, Fig. S3).

We next investigated whether AsiDNA can inhibit telomere fusions. Using a single molecule telomere fusion assay, targeting multiple chromosome ends (6), we compared the presence of fusions in treated and untreated HCT116-DNhTERT for both clones at every passage during crisis (Fig. 4A and B). We examined fusions involving 17p, XpYp and the 21q family of telomeres ends that comprises 12 related chromosome ends (6). We analysed a total of  $1.25 \times 10^6$  and  $1.05 \times 10^6$  diploid genome equivalents for clone 4 and clone 8, respectively, in treated and untreated cells. The frequency of fusions in treated cells was statistically significantly lower than in untreated cells for both clones. Interestingly, the difference in fusion frequencies between AsiDNA treated and untreated cells was particularly marked during the first half of crisis and disappeared in the second half (Fig. 4B). The total frequency of fusions during crisis

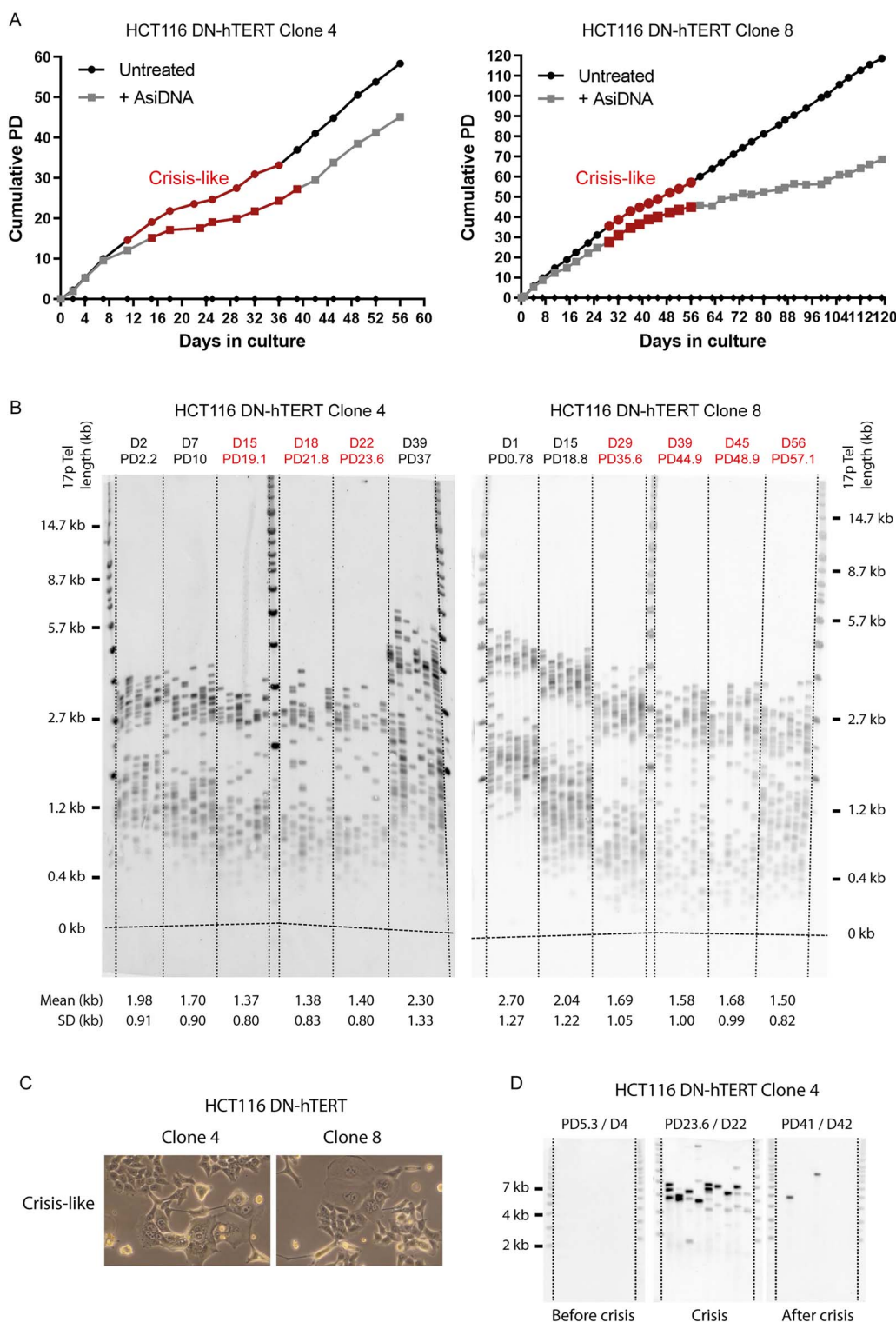


**Figure 1.** Impact of AsidDNA in HCT116 cells experiencing a telomere-driven crisis. (A) Growth curves plotting cumulative PDs from the first passage and days in culture of untreated and AsidDNA-treated HCT116-DNhTERT for two independent clones. The period of crisis and the PD points where telomere fusions are detected are shown in red. Treatment was renewed at every passage, every 3–4 days, as indicated by black diamonds on the x axis. (B) Single Telomere Length Analysis (STELA) of 17p telomere for both clones. Mean telomere length and standard deviation are shown below. PD and corresponding day points analysed are indicated above. PD/day points in red designate crisis and the presence of fusions. (C) Representative images of both HCT116-DNhTERT clones during crisis, illustrating a change in morphology that is characterized by enlarged and multinuclear cells. (D) Telomere fusion assay targeted at XpYp, 17p and 21q family telomeres in HCT116-DNhTERT before, during and after crisis. The PD/day points are indicated above.

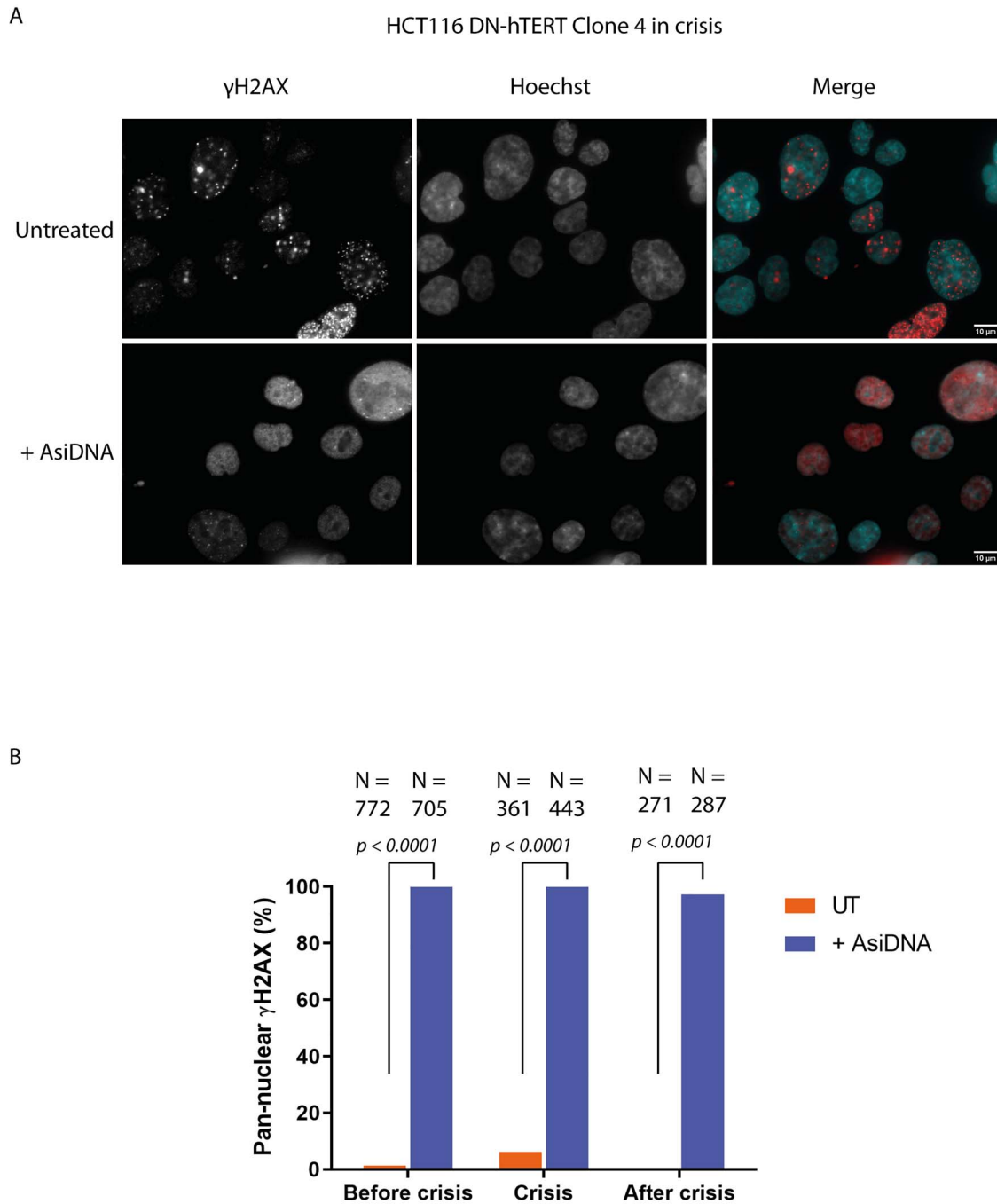


**Figure 2.** AsiDNA induces a pan nuclear phosphorylation of H2AX in HCT116-DNhTERT cells before and during crisis. (A) Immunostaining of  $\gamma$ -H2AX in untreated cells (D22) and AsiDNA treated cells (D22, 4 days after treatment), during crisis. DNA was stained with Hoechst. DNA is cyan and  $\gamma$ -H2AX is red in the combined image. (B) Quantification of the nuclei displaying a pan-nuclear  $\gamma$ -H2AX staining in cells before crisis (D10), during crisis (D18 and D22) and after crisis (D39). The total number of nuclei counted is indicated above. Statistical significance was determined using Fisher's exact test.

decreased from  $1.76 \times 10^{-4}$  in untreated cells to  $1.28 \times 10^{-4}$  in treated cells (chi-square test,  $P=0.0025$ ) for clone 4 and from  $4.29 \times 10^{-4}$  to  $3.16 \times 10^{-4}$  (chi-square test,  $P < 0.0001$ ) for clone 8. This represents a 1.38-fold decrease in the frequency of fusions detected for clone 4 and a 1.36-fold decrease for clone 8. Taken together, these results indicate that in HCT116-DNhTERT cells, AsiDNA decreases the frequency of telomere fusions without affecting the rate of telomere erosion.

#### AsiDNA does not significantly impact the choice of the repair pathway involved in telomere fusions during crisis

Since AsiDNA reduced the frequency of telomere fusions during crisis, we next wanted to investigate whether AsiDNA could also affect the choice of the repair pathway involved in fusions between short dysfunctional telomeres. The nature of the sequence at the fusion point is indicative of the repair

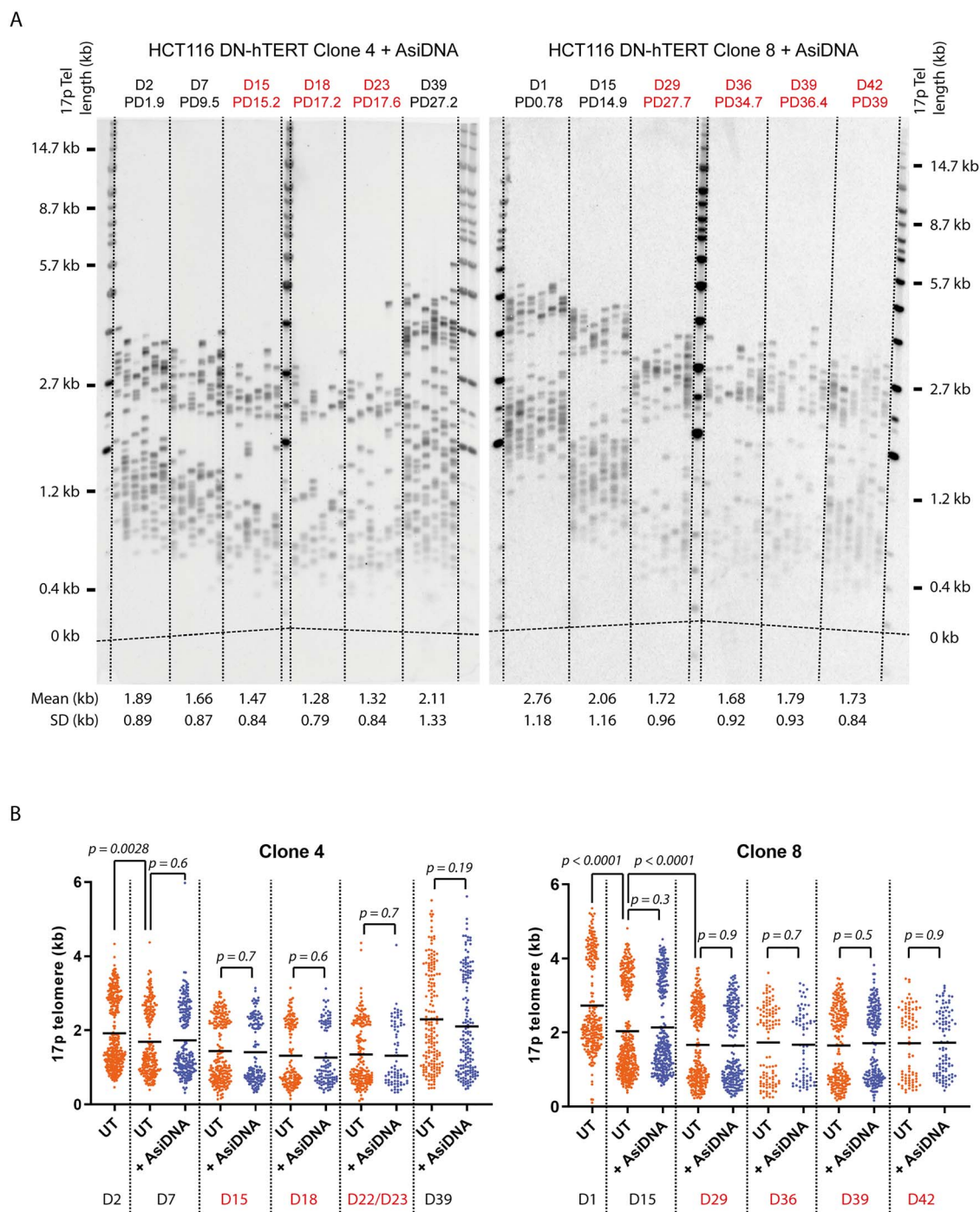


**Figure 3.** AsiDNA does not affect telomere erosion in HCT116-DNhTERT cells. (A) 17p STELA for both HCT116-DNhTERT clones treated with AsiDNA at the indicated PD/day points. Mean telomere length and standard deviation are shown below. PD/day points in red designate crisis and the presence of fusions. (B) 17p telomere length distributions in untreated versus AsiDNA treated HCT116-DNhTERT cells for both clones at the indicated day points. Day points in red designate crisis and the presence of fusions. Statistical significance was determined using Student's *t* test. (Mean).

mechanism involved (i.e. presence or not of microhomologies, deletions, insertions) (8,18). We therefore isolated and sequenced across the fusion point a total of 52 fusion events for the treated cells and 69 for the controls (Fig. 5A). Interestingly, the profiles of XpYp-17p fusions and 21q-17p/XpYp fusions were different in HCT116-DNhTERT cells, with 45.8% of XpYp-17p fusions containing telomere repeats on both sides of the fusion point and all of 21q-17p/XpYp fusions harbouring deletions

on one or both sides of the fusion point ( $P < 0.0001$ , Fisher's exact test) (Fig. 5B). The same difference in the profile between XpYp-17p fusions and 21q-17p/XpYp fusions was observed in the treated cells ( $P = 0.0164$ , Fisher's exact test) (Fig. 5B). However, the percentage of XpYp-17p fusions containing either telomeric repeats or subtelomeric deletions on both sides of the fusion point was lower in treated cells compared with untreated cells and the number of fusions containing deletions on either side of

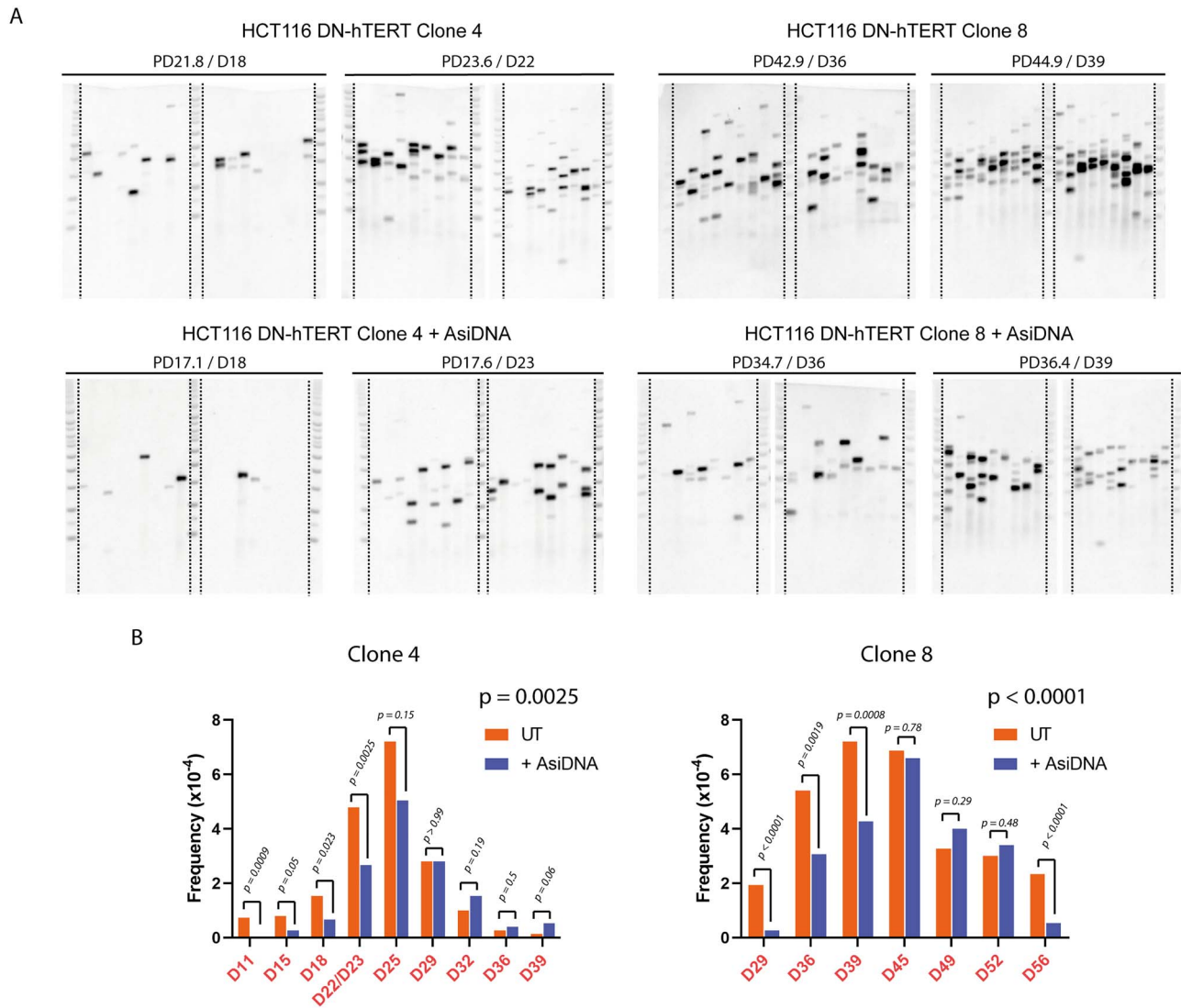


**Figure 4.** AsidDNA reduces the frequency of telomere fusions during crisis. (A) Telomere fusion assay targeting 17p, XpYp and 21q family telomeres in untreated and AsidDNA treated HCT116-DN-hTERT at the indicated PD/day points during crisis for both clones. (B) Frequency of telomere fusion events involving 17p chromosome end in untreated and AsidDNA treated HCT116-DN-hTERT during the entire crisis period, for both clones. The statistical comparison between the total frequency of fusions during crisis in untreated versus AsidDNA treated cells was determined by the chi-square test and the p values for each clone are indicated above each graph ( $P = 0.0025$  for clone 4 and  $P < 0.0001$  for clone 8). The individual P values for the statistical comparison between the fusion frequencies at each day point are also indicated (chi-square test).

the fusion point was higher in treated cells ( $P = 0.0189$ , Fisher's exact test) (Fig. 5B).

The proportion of XpYp-17p fusions and 21q-17p/XpYp fusions with microhomologies or insertions at the fusion point was similar in AsidDNA-treated and untreated cells ( $P = 0.46$ , Fisher's exact test, and  $P > 0.99$ , Fisher's exact test, respectively) (Fig. 5C). Nonetheless, there was a slight increase, which was not statistically significant, in the proportion of XpYp-17p fusions that used microhomologies in treated cells compared with untreated cells ( $P = 0.75$ , Fisher's exact test) (Fig. 5C). There were no significant differences, however, in the size of subtelomeric deletions, microhomologies and insertions at the fusion points of XpYp-17p and 21q-17p/XpYp fusions in treated cells compared with untreated cells (Fig. 5D–F).

Our investigation of the sequence of telomere fusion suggests that treatment with AsidDNA does not significantly impact the

relative utilization of DSB repair pathways involved in the fusion of short dysfunctional telomeres.

## Discussion

AsidDNA is a DNA repair inhibitor that acts by mimicking a DSB and hijacking the recruitment of proteins involved in various DNA repair pathways (i.e. NHEJ, HR, BER and SSBR) (19,20). During a telomere-driven crisis, chromosome ends are not protected and are recognized as DSBs by the repair machinery, leading to the phosphorylation of telomeric histone H2AX. The repair of unprotected telomeres results in end-to-end chromosome fusions and involves both A-NHEJ and C-NHEJ. Our data show that AsidDNA also leads to a pan-nuclear H2AX phosphorylation in cells in crisis. And this is associated with a reduction in the frequency of telomere fusions, which is independent of an effect on telomere erosion. There were no

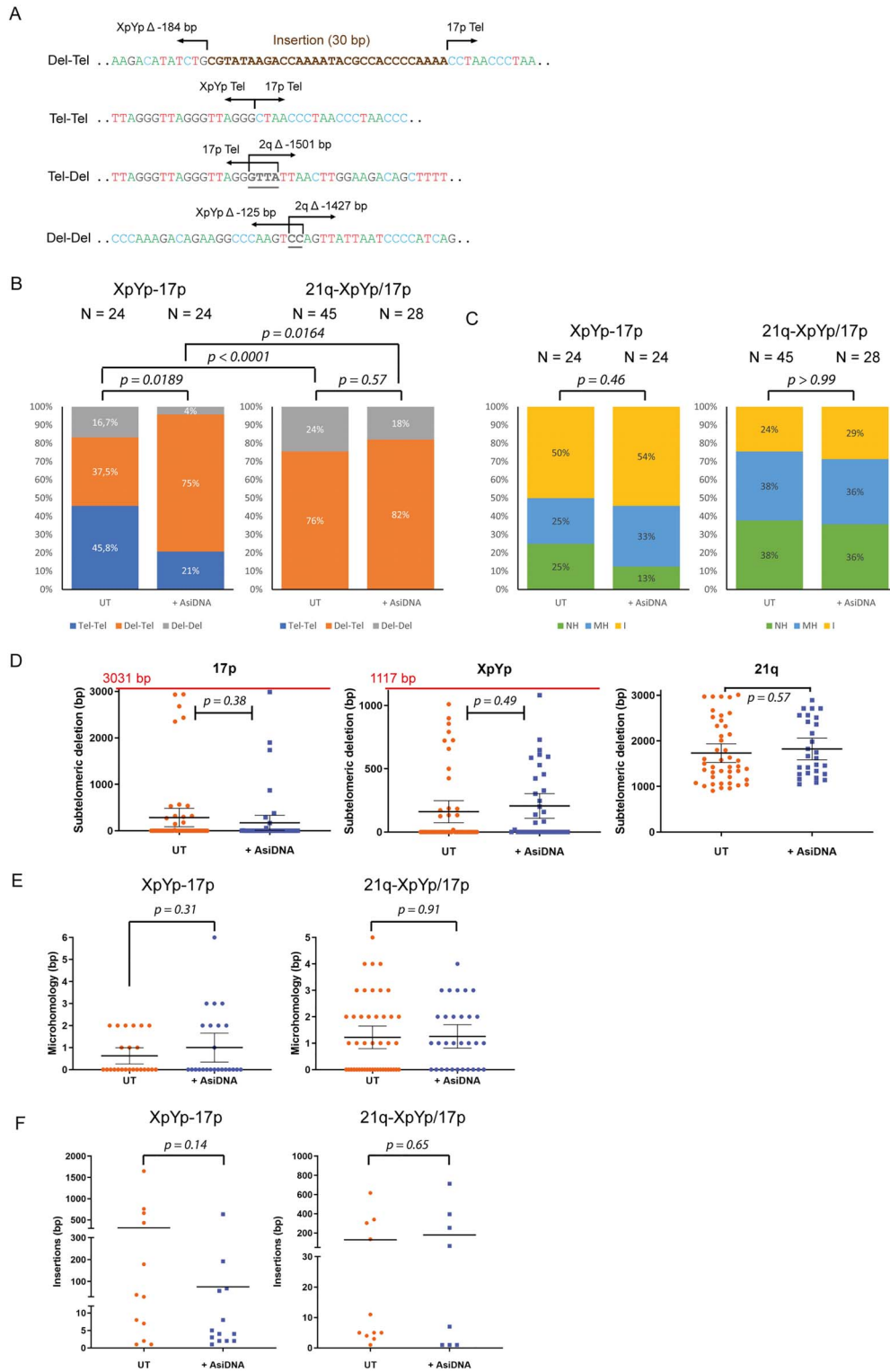


**Figure 5.** AsidNA does not significantly impact the molecular profile of telomere fusions. (A) Examples of DNA sequences of telomere fusion events in clone 4. The two participating telomeres are indicated together with the extent of deletion in the subtelomeric DNA. Insertions at the fusion point are shown in brown. Homology at the fusion point is in grey bold and underlined. (B) Profiles of XpYp-17p and 21q-XpYp/17p fusions in untreated and AsidNA treated HCT116-DNhTERT clone 4 cells. Tel-Tel refers to fusion events with telomere repeats on both sides of the fusion point. Del-Tel refers to fusion events with subtelomeric deletion on one side of the fusion point and telomere repeats on the other side. Del-Del refers to fusion events with deletions on both sides of the fusion point. The total number of fusions analysed is indicated above. The difference between the proportions of Del-Tel, for XpYp-17p fusions, in untreated cells compared with treated cells was assessed by Fisher's exact test ( $P = 0.0189$ ). The comparison of Del-Tel and Del-Del proportions, for 21q-XpYp/17p fusions, between untreated and treated cells was assessed by Fisher's exact test ( $P = 0.57$ ). The difference between the profiles of XpYp-17p fusions and 21q-XpYp/17p for both untreated and treated cells (Tel-Tel proportions versus Del-Tel and Del-Del) was assessed by Fisher's exact test ( $P < 0.0001$  for untreated and  $P = 0.0164$  for treated cells). (B) Proportion of XpYp-17p or 21q-XpYp/17p fusions with No homology

major differences in the profiles of the fusion events analysed, indicating that AsiDNA impacts both A-NHEJ and C-NHEJ pathways.

The profiles of XpYp-17p and 21q-17p/XpYp fusions were different in HCT116-DNhTERT cells. The majority of XpYp-17p fusions harboured telomere sequences on one or both sides of the fusion point while all 21q-17p/XpYp fusions displayed deletions on one or both sides of the fusion point. This suggests that XpYp-17p and 21q-17p/XpYp fusions might take place by different mechanisms. It could also indicate that XpYp and 17p telomeres were longer than the telomeres of the 21q family during crisis. Interestingly, in AsiDNA treated cells, XpYp-17p fusions were biased toward subtelomeric deletions on either side of the fusion point compared with untreated cells where the majority of fusions contained telomeric repeats. It has been shown that fusions within the telomere sequence use less microhomologies and that the proportion of events with no homology is higher in this type of fusion (8). Consistent with this result, the decrease of XpYp-17p fusions with telomere sequences on both sides of the fusions point, in AsiDNA-treated cells, was associated with a slight, but not significant, increase in the proportion of fusions using microhomologies. This suggests that in the case of XpYp-17p fusions AsiDNA might inhibit C-NHEJ and favour the use of A-NHEJ.

Interestingly, there seemed to be a slight, but not significant, increase in the number of XpYp-17p fusions with longer microhomologies and a slight, but not significant, decrease in the average size of insertions in AsiDNA treated cells. It would be interesting to confirm or infirm these differences and to fully explore the potential impact of AsiDNA on the molecular nature of telomere fusions. Such a comprehensive analysis would, however, require the analysis of a greater number of events, using next generation sequencing combined with high throughput sequence analysis (27).

However, there were no differences in the profiles of 21q-17p/XpYp fusions between AsiDNA-treated cells and untreated cells. This, on the contrary, indicates that both pathways are used for 21q-17p/XpYp fusions and that they are equally affected by AsiDNA. The reason for this apparent difference between XpYp-17p and 21q-XpYp/17p fusions is not clear. Both A-NHEJ and C-NHEJ are used for interchromosomal fusions between short dysfunctional telomeres. C-NHEJ mediated-fusions mostly, but not only, take place within the telomere repeat. A-NHEJ mediated-fusions seem to occur more often within the subtelomere sequence (8). Altogether, our data show a decrease in the frequency of fusion events in AsiDNA-treated cells but do not show major differences in their profiles compared with untreated cells. We conclude that AsiDNA might interfere with both A-NHEJ and C-NHEJ pathways in the fusion of short dysfunctional telomeres. However, the mechanism by which AsiDNA can affect A-NHEJ is not clear. AsiDNA binds and hyper-activates PARP, thus hijacking its function from bona fide damage sites. However, a recent study showed that PARP1 is not essential for A-NHEJ (28).

As discussed above, AsiDNA is thought to prevent short telomeres from fusing by inhibiting DNA repair. This hypothesis is supported by the fact that the decrease in fusion frequencies in AsiDNA treated cells was particularly marked during the first half of crisis and disappeared in the second half. The fact that most of the cells with fusions die subsequently might explain why after the peak of crisis the fusion frequencies of treated and untreated cells are similar.

An alternative, non-mutually exclusive possibility is that cells harbouring fusions preferentially die in the presence of AsiDNA, thus resulting in a reduction in fusion frequency. A possible explanation for the latter could be that, by hyperactivating a nonspecific DNA damage response, AsiDNA enhances cell death of cells already undergoing genomic instability. In support of this idea, sensitivity to AsiDNA has been associated with genome rearrangements (29).

Our data further characterized the action of AsiDNA in a context of a telomere-driven crisis, and could open the way for investigating the use of AsiDNA in the treatment of tumours that have short dysfunctional telomeres and/or are experiencing genomic instability.

## Materials and Methods

### Cell culture and cell growth experiment

HCT116-DNhTERT were grown in McCoy's 5A (modified) medium with GlutaMAX (Gibco, Dublin, Ireland), supplemented with 10% Foetal Calf Serum (Corning, Tewksbury, MA, USA) and 1% penicillin/streptomycin (Gibco). Cells were cultured in 10 cm Ø plates and passaged  $\approx$  every 3–4 days during the entire course of the experiment. Population Doublings (PDs) were calculated at every passage using the following equation:  $[\log(\text{total number of cells counted at day of passage}) - \log(\text{number of cells initially seeded at previous passage})] / \log 2$ . Cumulative Population Doubling is the total number of PDs at a given day point. At each reseeding the remaining cells were pelleted and snap-frozen for further analysis. Treated cells were grown in presence of 10  $\mu\text{g/ml}$  of AsiDNA and the treatment was renewed at every passage (every 3–4 days).

### Immunofluorescence

For immunofluorescence experiments, untreated and treated cells were reseeded, at the day of passage, on glass coverslips and allowed to grow for 3 or 4 days before being washed once with  $\times 1$  phosphate buffered saline (PBS, Gibco) and then fixed with 4% formaldehyde (Electron Microscopy Sciences, Hatfield, PA, USA). For clone 4, cells were reseeded at day 7 and fixed at day 10 (before crisis sample); reseeded at day 15 and fixed at day 18 and 22, respectively, (crisis samples) and reseeded at day 36 and fixed at day 39 (after crisis sample). For clone 8, cells were reseeded at day 18 and fixed at day 22 (before crisis sample); and reseeded at day 36 and fixed

(NH), Microhomologies (MH) or Insertions (I) at the fusion point in untreated and AsiDNA treated HCT116-DNhTERT clone 4 cells.  $\text{NH} \leq 1$  bp and  $\text{MH} > 1$  bp. The total number of fusion analysed is indicated above. The comparison of MH + I and NH proportions, for both XpYp-17p and 21q-XpYp/17p fusions, between untreated and treated cells was performed by Fisher's exact test ( $P = 0.46$  and  $P > 0.99$ ). (C) Scatter plots depicting the subtelomeric deletion from the start of the telomere repeat array, at 17p, XpYp and 21q family of related telomeres, in untreated and AsiDNA treated HCT116-DNhTERT clone 4 cells. The red line indicates the maximal deletion size that can be detected at 17p and XpYp with the telomere fusion assay. (Mean  $\pm$  95%CI). Unpaired t test and unpaired t test with Welch's correction were employed. (D) Scatter plots depicting the extent of homology at the fusion point of XpYp-17p or 21q-XpYp/17p fusions in untreated and AsiDNA treated HCT116-DNhTERT clone 4 cells. (Mean  $\pm$  95%CI). Unpaired t test and unpaired t test with Welch's correction were employed. (E) Scatter plots showing the size of the insertions at the fusion point of XpYp-17p or 21q-XpYp/17p fusions in untreated and AsiDNA treated HCT116-DNhTERT clone 4 cells. (Mean). Unpaired t test and unpaired t test with Welch's correction were employed.

at day 39 (crisis sample). Cells were permeabilized with 0.5% Triton  $\times$ 100 (Sigma, Saint-Louis, MO, USA) in  $\times$ 1 PBS for 10 min, then blocked with 5% FCS in  $\times$ 1 PBS-Tween-20 0.1% for 30 min. Cells were incubated with a 1/1000 dilution of primary antibody anti- $\gamma$ H2AX (clone JBW301, Millipore, Burlington, MA, USA) at room temperature for 45 min, then washed 3X with 1X PBS-Tween-20 0.1% and stained with an anti-mouse Alexa Fluor-488 secondary antibody (1/1000) (Molecular Probe, Eugene, OR, USA) at room temperature for 30 min. DNA was stained with Hoechst (Thermo-Fisher, Waltham, MA, USA). Cover slips were mounted with ProLong Gold (Invitrogen, Carlsbad, CA, USA). Images were captured with a Zeiss axio observer Z1 inverted microscope with a  $\times$ 63 objective (Oberkochen, Germany).

### Single telomere length analysis and telomere fusion assay

Genomic DNA from cells pellets was extracted using ENZA tissue DNA kit (Omegabiotek, Norcross, GA, USA). 17p and XpYp Telomere length analysis was undertaken using the modified STELA protocol (5,30). For the analysis of telomere fusions, we used the multiple-telomere protocol (6). Single-molecule fusion polymerase chain reactions (PCRs) were carried out with 17p6, XpYpM and 21q1 primers using 50 ng of DNA per reaction (6). Fusion events were detected by Southern blotting and hybridization with first the random-primed [ $\alpha^{32}$ P] labeled 17p telomere-adjacent probe then the XpYp telomere-adjacent probe and finally with the 21q telomere-adjacent probe (6). Fusion frequencies were calculated by counting the total number of fusions and dividing it by the number of input molecules. The number of input molecules was estimated from the total quantity of DNA used divided by the size of a diploid human genome. Telomere fusions were characterized at the molecular level after reamplification followed by Sanger sequencing, for clone 4 at days 18, 22/23, 29 and 32.

### Statistics

All statistical analyses were performed with GraphPad Prism 8 (San Diego, CA, USA) and all statistical tests were two-sided. Student's t test, unpaired t test with Welch's correction, Fisher's exact test and chi-square test were used.

### Supplementary Material

Supplementary Material is available at HMG online.

### Acknowledgements

We thank Professor Duncan Baird (Cardiff School of Medicine) for providing the two HCT116 DN-hTERT clones; and Dr Carine Giovannangeli (MNHN), Dr Jean-Paul Concordet (MNHN) and Dr Danièle Praseuth (MNHN) for comments on the manuscript.

*Conflict of Interest statement.* Jian-Sheng Sun is an AsiDNA patent holder (WO2008/034866; WO2011/161075).

### Funding

This work was supported by Muséum National d'Histoire Naturelle (MNHN); Institut national de la santé et de la recherche médicale (Inserm) and Centre national de la recherche scientifique (CNRS).

### References

- McClintock, B. (1939) The behavior in successive nuclear divisions of a chromosome broken at meiosis. *Proc. Natl. Acad. Sci.*, **25**, 405–416.
- Muller, J.H. (1938) The remaking of chromosomes. *Collect. Net.*, **13**, 181–198.
- Fagagna, F.d.'A.d., Reaper, P.M., Clay-Farrace, L., Fiegler, H., Carr, P., von Zglinicki, T., Saretzki, G., Carter, N.P. and Jackson, S.P. (2003) A DNA damage checkpoint response in telomere-initiated senescence. *Nature*, **426**, 194–198.
- Counter, C.M., Ailion, A.A., LeFeuvre, C.E., Stewart, N.G., Greider, C.W., Harley, C.B. and Bacchetti, S. (1992) Telomere shortening associated with chromosome instability is arrested in immortal cells which express telomerase activity. *EMBO J.*, **11**, 1921–1929.
- Capper, R., Britt-Compton, B., Tankimanova, M., Rowson, J., Letsolo, B., Man, S., Haughton, M. and Baird, D.M. (2007) The nature of telomere fusion and a definition of the critical telomere length in human cells. *Genes Dev.*, **21**, 2495–2508.
- Letsolo, B.T., Rowson, J. and Baird, D.M. (2010) Fusion of short telomeres in human cells is characterized by extensive deletion and microhomology, and can result in complex rearrangements. *Nucleic Acids Res.*, **38**, 1841–1852.
- Bhargava, R., Fischer, M. and O'Sullivan, R.J. (2020) Genome rearrangements associated with aberrant telomere maintenance. *Curr. Opin. Genet. Dev.*, **60**, 31–40.
- Jones, R.E., Oh, S., Grimstead, J.W., Zimbric, J., Roger, L., Heppel, N.H., Ashelford, K.E., Liddiard, K., Hendrickson, E.A. and Baird, D.M. (2014) Escape from telomere-driven crisis is DNA ligase III dependent. *Cell Rep.*, **8**, 1063–1076.
- Artandi, S.E., Chang, S., Lee, S.-L., Alson, S., Gottlieb, G.J., Chin, L. and DePinho, R.A. (2000) Telomere dysfunction promotes non-reciprocal translocations and epithelial cancers in mice. *Nature*, **406**, 641–645.
- Lin, T.T., Letsolo, B.T., Jones, R.E., Rowson, J., Pratt, G., Hewamana, S., Fegan, C., Pepper, C. and Baird, D.M. (2010) Telomere dysfunction and fusion during the progression of chronic lymphocytic leukemia: evidence for a telomere crisis. *Blood*, **116**, 1899–1907.
- Roger, L., Jones, R.E., Heppel, N.H., Williams, G.T., Sampson, J.R. and Baird, D.M. (2013) Extensive telomere erosion in the initiation of colorectal adenomas and its association with chromosomal instability. *JNCI J. Natl. Cancer Inst.*, **105**, 1202–1211.
- Letsolo, B.T., Jones, R.E., Rowson, J., Grimstead, J.W., Keith, W.N., Jenkins, G.J.S. and Baird, D.M. (2017) Extensive telomere erosion is consistent with localised clonal expansions in Barrett's metaplasia. *PLoS One*, **12**, e0174833.
- Lin, T.T., Norris, K., Heppel, N.H., Pratt, G., Allan, J.M., Allsup, D.J., Bailey, J., Cawkwell, L., Hills, R., Grimstead, J.W. et al. (2014) Telomere dysfunction accurately predicts clinical outcome in chronic lymphocytic leukaemia, even in patients with early stage disease. *Br. J. Haematol.*, **167**, 214–223.
- Strefford, J.C., Kadalayil, L., Forster, J., Rose-Zerilli, M.J.J., Parker, A., Lin, T.T., Heppel, N., Norris, K., Gardiner, A., Davies, Z. et al. (2015) Telomere length predicts progression and overall survival in chronic lymphocytic leukemia: data from the UK LRF CLL4 trial. *Leukemia*, **29**, 2411–2414.
- Simpson, K., Jones, R.E., Grimstead, J.W., Hills, R., Pepper, C. and Baird, D.M. (2015) Telomere fusion threshold identifies a poor prognostic subset of breast cancer patients. *Mol. Oncol.*, **9**, 1186–1193.

16. Hyatt, S., Jones, R.E., Heppel, N.H., Grimstead, J.W., Fegan, C., Jackson, G.H., Hills, R., Allan, J.M., Pratt, G., Pepper, C. et al. (2017) Telomere length is a critical determinant for survival in multiple myeloma. *Br. J. Haematol.*, **178**, 94–98.
17. Norris, K., Hillmen, P., Rawstron, A., Hills, R., Baird, D.M., Fegan, C.D. and Pepper, C. (2019) Telomere length predicts for outcome to FCR chemotherapy in CLL. *Leukemia*, **33**, 1953–1963.
18. Brambati, A., Barry, R.M. and Sfeir, A. (2020) DNA polymerase theta (Pol $\theta$ ) – an error-prone polymerase necessary for genome stability. *Curr. Opin. Genet. Dev.*, **60**, 119–126.
19. Quanz, M., Berthault, N., Roulin, C., Roy, M., Herbette, A., Agrario, C., Alberti, C., Jossierand, V., Coll, J.-L., Sastre-Garau, X. et al. (2009) Small-molecule drugs mimicking DNA damage: a new strategy for sensitizing Tumors to radiotherapy. *Clin. Cancer Res.*, **15**, 1308–1316.
20. Croset, A., Cordelières, F.P., Berthault, N., Buhler, C., Sun, J.-S., Quanz, M. and Dutreix, M. (2013) Inhibition of DNA damage repair by artificial activation of PARP with siDNA. *Nucleic Acids Res.*, **41**, 7344–7355.
21. Berthault, N., Maury, B., Agrario, C., Herbette, A., Sun, J.-S., Peyrieras, N. and Dutreix, M. (2011) Comparison of distribution and activity of nanoparticles with short interfering DNA (Dbait) in various living systems. *Cancer Gene Ther.*, **18**, 695–706.
22. Thierry, S., Jdey, W., Alculumbre, S., Soumelis, V., Noguez-Hellin, P. and Dutreix, M. (2017) The DNA repair inhibitor Dbait is specific for malignant hematologic cells in blood. *Mol. Cancer Ther.*, **16**, 2817–2827.
23. Herath, N.I., Berthault, N., Thierry, S., Jdey, W., Lienafa, M.-C., Bono, F., Noguez-Hellin, P., Sun, J.-S. and Dutreix, M. (2019) Preclinical studies comparing efficacy and toxicity of DNA repair inhibitors, Olaparib, and AsiDNA, in the treatment of carboplatin-resistant Tumors. *Front. Oncol.*, **9**, Article 1097.
24. Biau, J., Chautard, E., Berthault, N., de Koning, L., Court, F., Pereira, B., Verrelle, P. and Dutreix, M. (2019) Combining the DNA repair inhibitor Dbait with radiotherapy for the treatment of high grade glioma: efficacy and protein biomarkers of resistance in preclinical models. *Front. Oncol.*, **9**, Article 549.
25. Le Tourneau, C., Dreno, B., Kirova, Y., Grob, J.J., Jouary, T., Dutriaux, C., Thomas, L., Lebbé, C., Mortier, L., Saiag, P. et al. (2016) First-in-human phase I study of the DNA-repair inhibitor DT01 in combination with radiotherapy in patients with skin metastases from melanoma. *Br. J. Cancer*, **114**, 1199–1205.
26. Arnoult, N. and Karlseder, J. (2015) Complex interactions between the DNA-damage response and mammalian telomeres. *Nat. Struct. Mol. Biol.*, **22**, 859–866.
27. Liddiard, K., Ruis, B., Takasugi, T., Harvey, A., Ashelford, K.E., Hendrickson, E.A. and Baird, D.M. (2016) Sister chromatid telomere fusions, but not NHEJ-mediated interchromosomal telomere fusions, occur independently of DNA ligases 3 and 4. *Genome Res.*, **26**, 588–600.
28. Harvey, A., Mielke, N., Grimstead, J.W., Jones, R.E., Nguyen, T., Mueller, M., Baird, D.M. and Hendrickson, E.A. (2018) PARP1 is required for preserving telomeric integrity but is dispensable for A-NHEJ. *Oncotarget*, **9**, 34821–34837.
29. Jdey, W., Thierry, S., Popova, T., Stern, M.-H. and Dutreix, M. (2017) Micronuclei frequency in Tumors is a predictive biomarker for genetic instability and sensitivity to the DNA repair inhibitor AsiDNA. *Cancer Res.*, **77**, 4207–4216.
30. Baird, D.M., Rowson, J., Wynford-Thomas, D. and Kipling, D. (2003) Extensive allelic variation and ultrashort telomeres in senescent human cells. *Nat. Genet.*, **33**, 203–207.